Alexandria Engineering Journal 92 (2024) 92–101

Contents lists available at ScienceDirect

Alexandria Engineering Journal

journal homepage: www.elsevier.com/locate/aej

Original Article

Numerical analysis for second order differential equation of reaction-diffusion problems in viscoelasticity

Sekar Elango [a], L. Govindarao [a], J. Mohapatra [b], R. Vadivel [c], Nien-Tsu Hu [d,*]

[a] Department of Mathematics, Amrita School of Physical Science, Amrita Vishwa Vidyapeetham, Coimbatore, Tamilnadu, 641112, India
[b] Department of Mathematics, NIT Rourkela, Rourkela, Odisha, 769008, India
[c] Department of Mathematics, Faculty of Science and Technology, Phuket Rajabhat University, Phuket-83000, Thailand
[d] Graduate Institute of Automation Technology, National Taipei University of Technology, Taipei 10608, Taiwan

ARTICLE INFO

Keywords:
Singular perturbation
Reaction-Diffusion
Boundary layer
Central difference scheme
Uniform convergence

ABSTRACT

This study uses numerical methods to solve a specific type of reaction-diffusion problem arising in viscoelasticity (singularly perturbed Fredholm integro-differential equations). These equations are challenging because they exhibit ‘boundary layers’ near the edges of the area of interest. To approximate solutions, a technique known as a second-order scheme is used for derivatives, and the trapezoidal rule is used for integral terms. This is done on non-standard grids known as Shishkin-type meshes. We found that this numerical method and its rate of improvement (or convergence) are both of the second order, which means they improve consistently as the calculations continue. This improvement rate remains consistent even when dealing with small parameters in the equations. In addition, a post-processing method is used to enhance the rate of convergence from second order to almost fourth order, indicating a significant improvement in the speed and accuracy of the solutions. The practical effectiveness of these methods is confirmed through performance testing of the numerical scheme.

1. Introduction

Singularly perturbed problems (SPPs) arise in various fields of science and engineering when there are multiple scales of interest and one scale is significantly smaller or larger than the others. In the context of viscoelasticity, which deals with materials exhibiting both elastic and viscous behavior, singular perturbation problems often occur when there is a notable separation between the characteristic timescales or lengthscales of different phenomena. Viscoelastic materials exhibit time-dependent behavior, and the governing equations typically involve ordinary differential equations. Singular perturbation analysis can be applied to simplify and analyze these problems in certain limits. Here are some aspects of viscoelasticity where singular perturbation problems may arise.

Time Scales: The viscoelastic response of materials often involves multiple timescales. For example, the elastic response may occur on a much faster timescale than the viscous response. Singular perturbation methods can be used to analyze the behavior of the material in the limit of rapid elastic deformation. Boundary Layers: In some viscoelastic problems, boundary layers may develop where the material response undergoes rapid changes. The behavior of the material in these boundary layers may be analyzed using singular perturbation techniques. Stiffness Ratios: Singular perturbation methods can be applied when there is a large contrast in the stiffness of different components of the material. For instance, if the elastic modulus is much larger than the viscous modulus, the analysis might be simplified using perturbation methods. Geometry: Singular perturbation problems can also arise in viscoelasticity with significant geometric variations. For example, when a thin layer of viscoelastic material is placed on a rigid substrate, the behavior near the interface may require a separate analysis. High Frequencies: In the high-frequency limit, the elastic response dominates over the viscous response. Singular perturbation methods can be employed to extract the leading-order behavior in this limit. Analyzing singularly perturbed problems in viscoelasticity often involves developing asymptotic expansions, identifying the dominant terms in different limits, and constructing matched asymptotic expansions to bridge the different scales. The goal is to obtain simplified models that capture the essential physics in various limiting cases.

Suppose the most excellent derivative term in a differential equation (DEs) is multiplied by a tiny parameter $\varepsilon \in (0, 1)$. In that case, this parameter is said to be a singular perturbation parameter and the DEs

* Corresponding author.
E-mail address: nthu@ntut.edu.tw (N.-T. Hu).

https://doi.org/10.1016/j.aej.2024.02.046
Received 5 January 2024; Received in revised form 11 February 2024; Accepted 22 February 2024
Available online 4 March 2024

are called singularly perturbed differential equations (SPDEs). Due to the presence of the perturbation parameter, layers occur on the boundaries, named boundary layers. These SPDEs have a lot of applications in biology, ecology, physical sciences and other areas. For example, the one-dimensional groundwater flow and solute transport problem is governed by the following equation:

$$y_t(s,t) = \varepsilon z_{ss}(s,t) - \upsilon y_x(s,t) - \lambda y(s,t),\ s > 0,\ t > 0.$$

It explains how water and solutes flow through the unsaturated zone [10], where the time is t, the horizontal distance is s and both quantities are positive and measured to the right of the soil's center.

In many scientific domains, including engineering, biology, physics, chemistry, potential theory, electrostatics, finance, theory of elasticity, fluid dynamics, astronomy, economics, heat and mass transfer, and other subjects, Fredholm integro-differential equations (FIDEs) are extremely important (see, [2,3,7,14,23,28]. However, Obtaining precise FIDEs solutions is extremely challenging. As a result, numerical methods are crucial for resolving these problems in [5,6,14,28]. As an example, Green and Stech's proposal was made in [13]; provides a type of single-species population model where species can spread throughout the past time periods $[t - \tau_0, t]$.

$$y_t(s,t) = D y_{ss}(s,t) + r y(s,t)\left(\int_{-\tau_0}^{0} y(s,t+p)\,d\iota(p)\right),\ s > 0,\ t > 0,$$

with $y(s,t) = y_0(s,t)$, $-t \in [\tau_0,\ 0]$, $s \in (0,\pi)$ and $y(0,t) = y(\pi,t) = 0$, $t > 0$.

Polymer rheology, population dynamics, and mathematical models of glucose tolerance all use singularly perturbed Fredholm integro-differential equations (SPFIDEs). For more applications of SPFIDEs, can cite Lodge et al. [19]; De Gaetano and Arino [9]; Brunner and van der Houwen [4]; Jerri [15]; Particularly, Nefedov and Nikitin's optimum control issues offer the singularly perturbed Fredholm integral equation [25]. There have been some asymptotic solutions to this issue mentioned in (Lange and Smith [17]; Nefedov and Nikitin [25]). A class of singularly perturbed partial integro-differential equations in viscoelasticity is given by,

$$\rho u^{\rho}_{tt}(t,x) = \varepsilon u^{\rho}_{xx}(t,x) + \int_{-\infty}^{t} a(t-s) u^{\rho}_{ss}(s,x)\,ds + \rho g(t,x) + f(x),$$

The theory and approximate numerical solution of SPFIDEs are still at the initial stage. In recent years, various numerical methods have been proposed for first-order SPFIDEs on uniform and non-uniform meshes in [1,12,16]. In [8,11] discussed a second order SPFIDEs on Shishkin meshes. In [26,27,29–33] discussed various second-order SPPs with delay and their boundary conditions are integral boundary conditions; our objective is to present an effective numerical solution for the following problem using the motivation from this research.

The singularly perturbed Fredholm integro-differential equations (SPFIDEs) are of the form

$$\begin{aligned} &Lu(x) := L_1 u(x) + L_2 u(x) = f(x),\ x \in (0,1) = \Omega,\\ &u(0) = A, \quad u(l) = B, \end{aligned} \tag{1.1}$$

where $L_1 u = -\varepsilon u'' + a(x)u$, $L_2 u = -\lambda \int_0^1 K(x,s)u(s)\,ds$ and $\gamma > K(x,s) \in L^2[0,1]$. It is assumed that $a(x) \ge \beta > \lambda\gamma > 0$, where λ is a positive constant. Under the assumption stated above, the reaction-diffusion problem (1.1) has boundary layers that are close to $x = 0$ and $x = 1$.

Recently Durmaz et al. solved the problem (1.1) in [11] by using a fitted homogeneous type difference scheme on a Shishkin mesh then they obtained the non optimal second order rate of convergence. This article aims to solve numerically the problem (1.1) by using central difference scheme for second order derivative and composite trapezoidal rule for integral part on fitted meshes (Shishkin type meshes), firstly we obtain an optimal second order rate of convergence $\left(CN^{-2}\right)$ and secondly we apply the extrapolation technique then obtain the fourth order rate of convergence $\left(CN^{-4}\right)$.

The article is presented in the following sections: The analytical approach to the problem is examined in Section 2. Establish the non-uniform meshes and the computational analysis in Section 3. Section 4 introduces the Richardson extrapolation and its convergence analysis. Tables and graphs of numerical solutions are also presented in Section 5 and the conclusion of this article's Section 6. In this manuscript, we define C as a set of positive and ε are independent constants. The standard supremum norm, which is represented by $\|.\|$ in this case, is $\|\mathfrak{f}\|_{\mathfrak{D}} = \sup_{(y)\in\mathfrak{D}} |\mathfrak{f}(y)|$.

2. Properties of the solution

Theorem 2.1. *Any function $\Upsilon(x)$ with boundary points $\Upsilon(0)$, $\Upsilon(1)$ and differential operator $L\Upsilon(x)$ are non negatives, then $\Upsilon(x) \ge 0$, $\forall x \in \overline{\Omega} = [0,1]$.*

Proof. The proof follows [29] methodology.
Consider $t(x) = 1 + x$,
Note that, the function is non negative on $x \in \overline{\Omega}$, and also $Lt(x) > 0, \forall x \in \Omega$. Let

$$\mu = \max\left\{ \frac{-\Upsilon(x)}{t(x)} : x \in \overline{\Omega} \right\}.$$

Furthermore, $x_0 \in \overline{\Omega}$ such that $\Upsilon(x_0) + \mu t(x_0) = 0$ and $\Upsilon(x) + \mu t(x) \ge 0, \forall x \in \overline{\Omega}$. As a result, at $x = x_0$, the function $(\Upsilon + \mu t)$ reaches its minimum value. In the case that the theorem is false, $\mu > 0$ occurs.
Case (i): $x_0 = 0$ and $x_0 = 1$,

$$0 < (\Upsilon + \mu t)(x_0) = \Upsilon(x_0) + \mu t(x_0) = 0.$$

Case (ii): $x_0 \in \Omega$,

$$0 < L_1(\Upsilon + \mu t)(x_0) = -\varepsilon(\Upsilon + \mu t)''(x_0) + a(x_0)(\Upsilon + \mu t)(x_0) \le 0,$$

$$0 < L_2(\Upsilon + \mu t)(x_0) = -\lambda \int_0^1 K(x,s)(\Upsilon + \mu t)(s)\,ds \le 0.$$

It contradicts itself. □

Theorem 2.2. ***Stability result***
If $u(x)$ is the solution of the problem (1.1), then the solution and derivative of the solution of the problem are bounded by as follows:

(i) $\|u(x)\| \le C \max\left\{u(0), u(1), Lu(x)\right\}$.
(ii) $\|u^k\| \le C(1 + \varepsilon^{-k/2})$, *for* $k = 1,2,3,4$.

Proof. The proof is available in [20]. □

Lemma 2.3. *If the solution decomposition is given by, $u = v + w_L + w_R$, where v is smooth and w_L, w_R are singular components solution of (1.1), then, it holds*

(i) $|v^k(x)| \le C(1 + \varepsilon^{-(k-2)/2})$.
(ii) $|w_L^k| \le C\varepsilon^{-k/2} e^{-x\sqrt{\beta/\varepsilon}}$.
(iii) $|w_R^k| \le C\varepsilon^{-k/2} e^{-(1-x)\sqrt{\beta/\varepsilon}}$, *where* $k = 1,2,3,4$.

Proof. (i) The proof is available in [[20, Chapter 6 (page:48)]].
(ii) Consider $\psi^{\pm}(x) = Ce^{-x\sqrt{\beta/\varepsilon}} \pm w_L(x)$. Note that $\psi^{\pm}(0) \ge 0$ and

$\psi^{\pm}(1) \geq 0$.
We have

$$L\psi^{\pm}(x) = Ce^{-x\sqrt{\beta/\varepsilon}}\Big[\varepsilon(-\beta/\varepsilon) + a(x)\Big] - \lambda \int_0^1 CK(x,s)e^{-s\sqrt{\beta/\varepsilon}}ds \pm Lw_L(x) \geq Ce^{-x\sqrt{\beta/\varepsilon}}\Big[a(x) - \beta - \lambda\gamma\Big] \geq 0.$$

By Theorem 2.1, we have $\psi^{\pm}(x) \geq 0$ and thus

$$|w_L(x)| \leq Ce^{-x\sqrt{\beta/\varepsilon}}.$$

For the derivative bounds of the left singular component, the proof is the same as in [20], resulting in

$$|w_L^{(k)}(x)| \leq Ce^{-x\sqrt{\beta/\varepsilon}}\varepsilon^{-k/2}.$$

(iii) It can be proven similarly as in the previous case that

$$|w_R^{(k)}| \leq C\varepsilon^{-k/2}e^{-(1-x)\sqrt{\beta/\varepsilon}}. \quad \square$$

3. Nonuniform meshes

3.1. Shishkin mesh (S-mesh)

The transition parameter σ is described as $\sigma = \min\left\{\frac{1}{4}, \frac{\sigma_0\sqrt{\varepsilon}}{\beta}\ln(N)\right\}$, where $\sigma_0 > 0$ is user choice constant and assume that $\sqrt{\varepsilon} \leq N^{-1}$. The detailed S-mesh can find in [20,34]. The mesh points must be defined as $\overline{\Omega}^N = \{x_0, x_1, x_2, \dots x_n\} \in [0,1]$, where

$$x_i = \begin{cases} iH_1, & \text{for} \quad i = 0, \dots, \frac{N}{4}, \\ \sigma + \left(\frac{i}{N} - \frac{1}{4}\right)H_2, & \text{for} \quad i = \frac{N}{4}+1, \dots, \frac{3N}{4}, \\ 1 - (N-i)H_1, & \text{for} \quad i = \frac{3N}{4}+1, \dots, N, \end{cases}$$

here, $H_1 = 4\sigma/N$, $H_2 = 2(1-2\sigma)$. The step size in space given by $h_i = x_i - x_{i-1}$, for $i = 1, \dots, N$.

Bakhvalov-Shishkin mesh (BS-mesh)

For the detailed construction of the B-S mesh one can cite [18]. The mesh is

$$x_i = \begin{cases} \frac{\sigma_0\sqrt{\varepsilon}}{\beta}\ln\left(\vartheta(\frac{i}{N}) + 1\right), & \text{for} \quad i = 0, \dots, N/4, \\ \sigma_1 + \left(\frac{4i}{N} - 1\right)(1/2 - \sigma_1), & \text{for} \quad i = \frac{N}{4}+1, \dots, \frac{3N}{4}, \\ 1 + \frac{\sigma_0\sqrt{\varepsilon}}{\beta}\ln\left(\vartheta(1-\frac{i}{N}) + 1\right), & \text{for} \quad i = \frac{3N}{4}+1, \dots, N, \end{cases}$$

where, $\sigma_1 = \min\left\{\frac{1}{4}, \frac{\sigma_0\sqrt{\varepsilon}}{\beta}\ln\min\{\varepsilon^{-1}, N\}\right\}$ and $\vartheta = 4\Big(\exp\big(-\beta\sigma_1/(\sigma_0\sqrt{\varepsilon})\big) - 1\Big)$. We take the step size as $h_i = x_i - x_{i-1}$.

3.2. Numerical scheme

The forward and backward center difference operators are defined as follows, where mesh function ϕ_i is given by,

$$D_x^+\phi_i = \frac{\phi_{i+1}-\phi_i}{h_{i+1}}, \quad D_x^-\phi_i = \frac{\phi_i - \phi_{i-1}}{h_i}, \quad D_x^0\phi_i = \frac{\phi_{i+1}-\phi_{i-1}}{h_{i+1}+h_i},$$

and the approximate second-order operator is defined as

$$D_x^+D_x^-\phi_i = \frac{2}{h_i + h_{i+1}}\left(\frac{\phi_{i+1}-\phi_i}{h_{i+1}} - \frac{\phi_i - \phi_{i-1}}{h_i}\right),$$

where $\phi_i = \phi(x_i)$. We discretize the problem (1.1) by the central difference scheme for second order derivative and a trapezoidal method for an integral part on the domain $\Omega^N = \{x_1, x_2, \dots x_{n-1}\}$.

The proposed numerical scheme is given in the following form:

$$\begin{cases} L^N U_i \equiv \left(L_1^N + L_2^N\right)U_i = f_i, \text{for} \quad i = 1, \dots, N-1, \\ U_0 = \theta_1, \quad U_N = \theta_2, \end{cases} \tag{3.1}$$

where,

$$L_1^N U_i = -\varepsilon D_x^+D_x^- U_i + a_i U_i,$$

$$L_2^N U_i = -\lambda \sum_{j=0}^{N} \tau_j K_{i,j} U_j,$$

$$\tau_0 = \frac{h_0}{2}, \quad \tau_j = \frac{h_j + h_{j+1}}{2}, \quad j = 1, 2, \dots, N-1, \; \tau_N = \frac{h_N}{2}.$$

The approximate solution of (3.1) is $U_i = U(x_i)$, $a_i = a(x_i)$, $f_i = f(x_i)$ and $x_i \in \Omega^N$.

Theorem 3.1. *Any function $\Upsilon(x_i)$ with boundary points $\Upsilon(x_0)$, $\Upsilon(x_N)$ and operator $L^N\Upsilon(x_i)$ are non negatives, then $\Upsilon(x_i) \geq 0$, $\forall x_i \in \overline{\Omega}^N$.*

Proof. Consider $t(x_i) = 1 + x_i$,
Note that, the function is non negative on $x_i \in \overline{\Omega}^N$, and also $L^N t(x_i) > 0, \forall x_i \in \Omega^N$. Let

$$\mu = \max\left\{\frac{-\Upsilon(x_i)}{t(x_i)} : x_i \in \overline{\Omega}^N\right\}.$$

Furthermore, $x_k \in \overline{\Omega}^N$ such that $\Upsilon(x_k) + \mu t(x_k) = 0$ and $\Upsilon(x_i) + \mu t(x_i) \geq 0, \forall x_i \in \overline{\Omega}^N$. As a result, at $x = x_k$, the function $(\Upsilon + \mu t)$ reaches its minimum attains. In the case that the theorem is false, $\mu > 0$ occurs.
Case (i): $x_k = x_0$ and $x_k = x_N$

$$0 < (\Upsilon + \mu t)(x_k) = \Upsilon(x_k) + \mu t(x_k) = 0$$

Case (ii): $x_k \in \Omega^N$

$$0 < L_1(\Upsilon + \mu t)(x_k) = -\varepsilon D_x^+D_x^-(\Upsilon + \mu t)(x_k) + a(x_k)(\Upsilon + \mu t)(x_k) \leq 0,$$

$$0 < L_2(\Upsilon + \mu t)(x_k) = -\lambda\Big[h_1 k_{i,1}(\Upsilon + \mu t)_1 + \dots + h_N k_{i,N}(\Upsilon + \mu t)_N\Big]. \leq -\lambda(\Upsilon + \mu t)_k\Big[h_1 k_{i,1} + \dots + h_N k_{i,N}\Big] \leq 0.$$

It contradicts itself. $\square$

Theorem 3.2. *(Discrete stability results): Let ϕ_i be any function that satisfies the following bound*

$$\Big|\phi_i\Big| \leq \frac{1}{\beta}\max_{1\leq j\leq N-1}\Big|L^N\phi_j\Big|.$$

Proof. One can prove this easily by using Theorem 3.1.

3.3. Error estimate for the difference schemes

Remark 1. Using the integral form of the truncation term and the composite trapezoidal rule on the range $[0,1]$:

$$\int_0^1 F(s)ds = \sum_{i=0}^{N} h_i F_i + R_N, \tag{3.2}$$

with $\tau_0 = \frac{h_1}{2}$, $\tau_i = \frac{h_i + h_{i+1}}{2}$, $\quad i = 1, 2, 3, ..., N-1$, $\tau_N = \frac{h_N}{2}$, and

$$R_N = \frac{1}{2}\sum_{i=1}^{N}\int_{x_{i-1}}^{x_i}(x_i-\xi)(x_{i-1}-\xi)F''(\xi)d\xi.$$

Then, using (3.2), it follows

$$\lambda\int_0^1 K(x_i,s)u(s)ds = \lambda\sum_{j=0}^{N} h_j K_{ij}u_j + R_i,$$

where,

$$R_i = \frac{\lambda}{2}\sum_{j=1}^{N}\int_{x_{j-1}}^{x_j}(x_j-\xi)(x_{j-1}-\xi)\frac{d^2}{d\xi^2}(K(x_i,\xi))u(\xi)d\xi,$$

$$|R_i| = \left|\frac{\lambda}{2}\sum_{j=1}^{N}\int_{x_{j-1}}^{x_j}(x_j-\xi)(x_{j-1}-\xi)\frac{d^2}{d\xi^2}(K(x_i,\xi))u(\xi)d\xi\right|,$$

$$\left|R_i\right| \le C\sum_{j=1}^{N}\int_{x_{j-1}}^{x_j}(x_j-\xi)(\xi-x_{j-1})(1+|u'(\xi)|+|u''(\xi)|)d\xi.$$

Theorem 3.3. *Let u and U be the solutions to (1.1) and (3.1) respectively; then, the following estimate is satisfied by the numerical scheme's error (3.1)*

$$\max_i\left|(u-U)(x_i)\right| \le \begin{cases} C\left((N^{-1}\ln N)^2\right) & \text{on S-mesh,}\\ CN^{-2} & \text{on B-S-mesh}\end{cases}$$

for $i = 1,\dots,N-1$.

Proof. The discrete solution U decomposed into smooth (V) and singular (W) components. The error can be written in the form

$$L^N(U-u) = L_1^N(U-u) + L_2^N(U-u).$$

By Miller [20],

$$L_1^N(U-u) \le C(N^{-1}\ln N)^2.$$

Now, for the operator L_2 it holds,

$$L_2^N(U-u) = L_2^N(V-v) + L_2^N(W-w) \le C(N^{-1}\ln N)^2.$$

Smooth components:

$$\begin{aligned} L_2^N(V_i-v_i) &= L_2^N(V(x_i)) - L_2^N(v(x_i))\\ &= \lambda\sum_{j=0}^{N}\tau_j K_{ij}V_j - \lambda\int_0^1 K(x,s)v(s)ds\\ &= \lambda\sum_{j=0}^{N}\tau_j K_{ij}v_j - \lambda\int_0^1 K(x_i,s)v(s)ds\\ &\le C\sum_{j=1}^{N}\int_{x_{j-1}}^{x_j}(x_j-\xi)(\xi-x_{j-1})(1+|v'(\xi)|+|v''(\xi)|)d\xi\\ &\le C\sqrt{\varepsilon}(h)\\ &\le CN^{-1}(h)\end{aligned}$$

$$L_2^N(V_i-v_i) \le CN^{-2}.$$

By using stability result, it follows

$$|V(x_i)-v(x_i)| \le CN^{-2}\ln N.$$

Singular components:

$$\begin{aligned} L_2^N(W_i-w_i) &= L_2^N(W(x_i)) - L_2^N(w(x_i))\\ &= \lambda\sum_{j=0}^{N}\tau_j K_{ij}W_j - \lambda\int_0^1 K(x_i,s)w(s)ds\\ &= \lambda\sum_{j=0}^{N}\tau_j K_{ij}W_j - \lambda\int_0^1 K(x_i,s)w(s)ds\\ &\le C\sum_{j=1}^{N}\int_{x_{j-1}}^{x_j}(x_j-\xi)(\xi-x_{j-1})(1+|w'(\xi)|+|w''(\xi)|)d\xi\\ &\le C\sum_{j=1}^{N}\int_{x_{j-1}}^{x_j}(x_j-\xi)(\xi-x_{j-1})(\frac{1}{\varepsilon})(e^{-x\sqrt{\beta/\varepsilon}}+e^{-(1-x)\sqrt{\beta/\varepsilon}})d\xi\\ &\le CN^{-1}\frac{h^3}{\varepsilon}\end{aligned}$$

$$L_2^N(W_i-w_i) \le CN^{-2}\ln^2 N.$$

By Stability results,

$$|W(x_i)-w(x_i)| \le CN^{-2}\ln^2 N.$$

Therefore,

$$|U(x_i)-u(x_i)| = |V(x_i)-v(x_i)| + |W(x_i)-w(x_i)| \le CN^{-2}\ln^2 N.$$

Similarly, on B-S mesh, we get

$$|U(x_i)-u(x_i)| = |V(x_i)-v(x_i)| + |W(x_i)-w(x_i)| \le CN^{-2}. \quad \square$$

4. Post process technique

We use the Richardson extrapolation approach to improve the accuracy of the numerical solution and convergence rate. The discrete problems (3.1) are first solved on the Shishkin type mesh $\overline{\Omega}^{2N}$, which is created by dividing each mesh interval of $\overline{\Omega}^{N}$ by a specified transition parameter. Consequently, the appropriate S-mesh nodes $\overline{\Omega}^{2N} = \{\widetilde{x}_i \in [0,1], 0=\widetilde{x}_0<\widetilde{x}_1<\cdots<\widetilde{x}_{2N-1}<\widetilde{x}_{2N}=1\}$ by

$$\widetilde{x}_i = \begin{cases} iH_1, & \text{for } 0\le i\le \frac{N}{2},\\ \sigma+\left(\frac{i}{N}-\frac{1}{4}\right)H_2, & \text{for } \frac{N}{2}+1\le i\le\frac{3N}{2},\\ 1-(N-i)H_1, & \text{for } \frac{3N}{2}+1\le i\le 2N,\end{cases}$$

and the B-S-mesh is

$$\widetilde{x}_i = \begin{cases} \frac{\sigma_0\sqrt{\varepsilon}}{\beta}\ln\left(\vartheta(\frac{i}{N})+1\right), & \text{for } 0\le i\le N/2,\\ \sigma_1+\left(\frac{4i}{N}-1\right)(1/2-\sigma_1), & \text{for } \frac{N}{2}+1\le i\le\frac{3N}{2},\\ 1+\frac{\sigma_0\sqrt{\varepsilon}}{\beta}\ln\left(\vartheta(1-\frac{i}{N})+1\right), & \text{for } \frac{3N}{2}+1\le i\le 2N.\end{cases}$$

Now, the similar way extrapolation as done in [22] and form Theorem 3.3, the error is

$$\begin{aligned}(u-U)x_i &= C\left((N^{-1}\ln N)^2\right)+o\left((N^{-1}\ln N)^2\right),\\ &= C(\tfrac{N^{-1}\sigma}{\rho_0\sqrt{\varepsilon}})^2+o\left((N^{-1}\ln N)^2\right),\end{aligned} \tag{4.1}$$

for $x_i\in\overline{\Omega}^N$. Let $\widetilde{U}(\widetilde{x}_i)$ represent the discrete problem's solution on the mesh $\overline{\Omega}^{2N}$ (see (3.1)). From Theorem 3.3, then

$$(\widetilde{U}^N-u)\widetilde{x}_i = C\left((2N)^{-2}(\tfrac{\sigma}{\rho_0\sqrt{\varepsilon}})^2\right)+o\left((N^{-1}\ln N)^2\right), \tag{4.2}$$

for $\widetilde{x}_i, \in \overline{\Omega}^{2N}$. Now, the elimination of $o(N^{-2})$ term from (4.1) and (4.2) produces the following better estimation

$$o\Big((N^{-1}\ln N)^2\Big) = u(x_i) - \frac{1}{3}\Big(4\widetilde{U}^N - U\Big)(x_i),\ x_i \in \overline{\Omega}^N. \tag{4.3}$$

So that we may extrapolate, we utilize the formula as

$$U_{exp}(x_i) = \frac{1}{3}\Big(4\widetilde{U}^N - U\Big)x_i, \quad x_i \in \overline{\Omega}^N. \tag{4.4}$$

Theorem 4.1. *Let U_{exp} represent the result of the Richardson extrapolation method (4.4) by solving the discrete problem (3.1) on two meshes $\overline{\Omega}^N$ and $\overline{\Omega}^{2N}$ and u be the solution of the continuous problem (1.1). Also, assume that $\sqrt{\varepsilon} \le N^{-1}$. Then we have the following error bound on*

$$\Big|U_{exp}(x_i) - u(x_i)\Big| \le \begin{cases} C\Big(N^{-4}\ln^4 N\Big), & \text{on S-mesh},\\ CN^{-4} & \text{on B-S-mesh}, \quad \text{for} \quad 1 \le i \le N-1. \end{cases}$$

Proof. The error can be written in the form

$$L^N(U_{exp} - u) = L_1^N(U_{exp} - u) + L_2^N(U_{exp} - u).$$

We have

$$L_1^N(U_{exp} - u) \le C(N^{-1}\ln N)^4,$$

the complete proof of this bound is available in [24] Now, To prove L_2 operator,

$$L_2^N(U_{exp} - u) = L_2^N(V_{exp} - v) + L_2^N(W_{exp} - w) \le C(N^{-1}\ln N)^4.$$

We decompose $\widetilde{U}$ on $\overline{\Omega}^{2N}$ as $\widetilde{U} = \widetilde{V} + \widetilde{W}$, where $\widetilde{W}$ is the layer component and $\widetilde{V}$ is smooth the layer on $\overline{\Omega}^{2N}$.

Error in smooth component:

$$L_2^N(V_i - v_i) = L_2^N(V(x_i)) - L_2^N(v(x_i)), \quad \text{for} \quad x_i \in \overline{\Omega}^N,$$

from the integral form of Taylor series expansion and using the derivative bounds as we have done in Theorem 3.3, we can prove

$$L_2^N(V_i - v_i) \le C\big(N^{-2} + N^{-4}\big),$$
$$L_2^N(V_i - v_i) \le CN^{-2} + O\big(N^{-4}\big),$$

from the stability result we can write

$$\Big|(V_i - v_i)\Big| \le CN^{-2} + O\big(N^{-4}\big) \quad \text{for} \quad x_i \in \overline{\Omega}^N. \tag{4.5}$$

Similarly we can obtain on $\overline{\Omega}^{2N}$,

$$\Big|(\widetilde{V}_i - v_i)\Big| \le C(2N)^{-2} + O\big(N^{-4}\big) \quad \text{for} \quad \widetilde{x}_i \in \overline{\Omega}^{2N}. \tag{4.6}$$

From the extrapolation formula (4.4), we have

$$\begin{aligned}(V_{exp} - v)(x_i) = &\quad \Big(\frac{1}{3}(4\widetilde{V} - V)(x_i)\Big) - v(x_i)\\ &= \frac{1}{3}\Big(4(\widetilde{V} - v) + (V - v)\Big)(x_i).\end{aligned}$$

From (4.5) and (4.6), we get

$$\Big|(V_{exp} - v)(x_i)\Big| = \Big|\frac{1}{3}\Big(4(\widetilde{V} - v) + (V - v)\Big)(x_i)\Big| \le CN^{-4}.$$

Layer components:

$$L_2^N(W_i - w_i) = L_2^N(W(x_i)) - L_2^N(w(x_i)), \quad \text{for} \quad x_i \in \overline{\Omega}^N,$$

from the integral form of Taylor series expansion and using derivative bounds as we have done in Theorem 3.3, then we have

$$L_2^N(V_i - v_i) \le C\big(N^{-2}(\ln N)^2 + N^{-4}\big),$$
$$L_2^N(W_i - w_i) \le CN^{-2}(\ln N)^2 + O\big(N^{-4}(\ln N)^4\big),$$

from the stability result we can write

$$\Big|(W_i - w_i)\Big| \le CN^{-2}(\ln N)^2 + O\big(N^{-4}(\ln N)^4\big) \quad \text{for} \quad x_i \in \overline{\Omega}^N. \tag{4.7}$$

Similarly on $\overline{\Omega}^{2N}$,

$$\Big|(\widetilde{V}_i - v_i)\Big| \le C(2N)^{-2}(\ln 2N)^2 + O\big(N^{-4}(\ln N)^2\big) \quad \text{for} \quad \widetilde{x}_i \in \overline{\Omega}^{2N}.$$
$$\Big|(\widetilde{W}_i - w_i)\Big| \le C(2N)^{-2}(\ln N)^2 + O\big(N^{-4}(\ln N)^2\big) \quad \text{for} \quad \widetilde{x}_i \in \overline{\Omega}^{2N}. \tag{4.8}$$

From the extrapolation formula (4.4), we can write

$$\begin{aligned}(W_{exp} - w)(x_i) = &\quad \Big(\frac{1}{3}(4\widetilde{V} - V)(x_i)\Big) - w(x_i)\\ &= \frac{1}{3}\Big(4(\widetilde{W} - w) + (W - w)\Big)(x_i).\end{aligned}$$

From (4.7) and (4.8), we get

$$\Big|(W_{exp} - w)(x_i)\Big| = \Big|\frac{1}{3}\Big(4(\widetilde{W} - w) + (W - w)\Big)(x_i)\Big| \le CN^{-4}(\ln N)^4.$$

Hence we obtain bound on S-mesh

$$\Big|U_{exp}(x_i) - u(x_i)\Big| \le CN^{-4}(\ln N)^4.$$

In a similar way we can prove the bound B-S mesh as

$$\Big|U_{exp}(x_i) - u(x_i)\Big| \le CN^{-4}.$$

For more details about B-S mesh, one can find in [21]. □

5. Computational simulations

The suggested method (3.1) is used to solve two test problems, and the results are presented in this section.

Example 5.1. Consider SPFIDEs below:

$$\begin{cases} -\varepsilon u''(x) + (2 - e^{-x})u(x) - 0.5\displaystyle\int_0^1 xu(s)ds = x\cos(x), \quad x \in (0,1),\\ u(0) = 1,\ u(1) = 0. \end{cases} \tag{5.1}$$

Example 5.2. Consider the following SPFIDE:

$$\begin{cases} -\varepsilon u''(x) + (1 + sin(\frac{\pi x}{2}))u(x) - 0.5\displaystyle\int_0^1 e^{1-xs}u(s)ds = \sqrt{1+x}, \quad x \in (0,1),\\ u(0) = -1,\ u(1) = 1. \end{cases} \tag{5.2}$$

The exact solutions are unknown for the Example 5.1 and Example 5.2. We apply the concept of the double mesh principle, which is defined as follows, to acquire the pointwise errors and to confirm the ε-uniform convergence: Assume that $\widetilde{U}(x_i)$ represents the numerical result achieved on the Shishkin-type mesh created with the fixed transition parameter. This mesh is based on the $\overline{\Omega}^{2N}$ grid.

Now, we determine the maximum wise error both before and after extrapolation for each ε by $E_\varepsilon^N = \max_{(x_i)\in\overline{\Omega}^N} |U(x_i) - \widetilde{U}(x_i, t_n)|$, and $E_\varepsilon^N = \max_{(x_i)\in\overline{\Omega}^N} |U_{exp}(x_i) - \widetilde{U}_{exp}(x_i)|$, together. The convergence in the corresponding order is defined by $P_\varepsilon^N = \log_2\left(\frac{E_\varepsilon^N}{E_\varepsilon^{2N}}\right)$. Here, the double mesh concept is used to derive the extrapolation solution for $\widetilde{U}_{exp}(x_i)$.

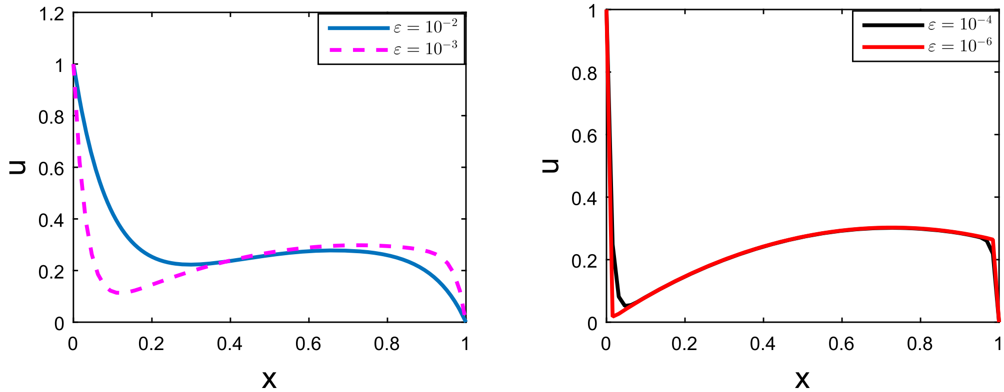

Fig. 1. Plots of the solutions for N = 64 of Example 5.1 on the S-mesh.

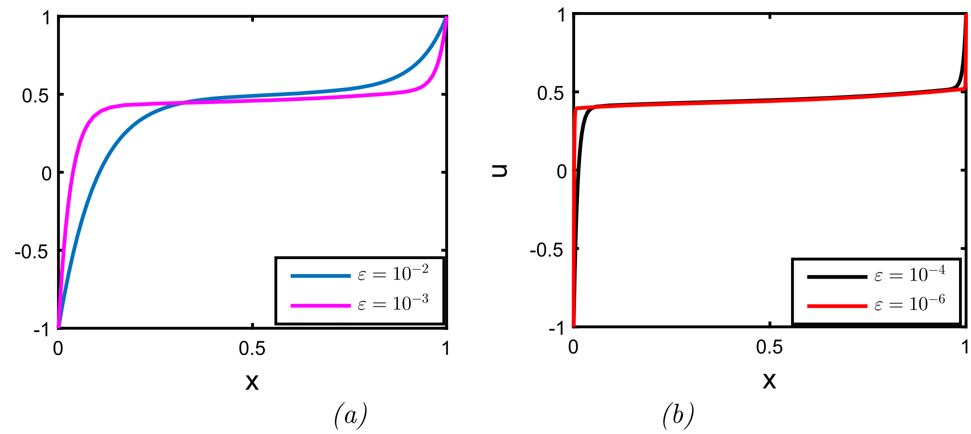

Fig. 2. Plots of the solutions for N = 64 of Example 5.2 on the B-S-mesh.

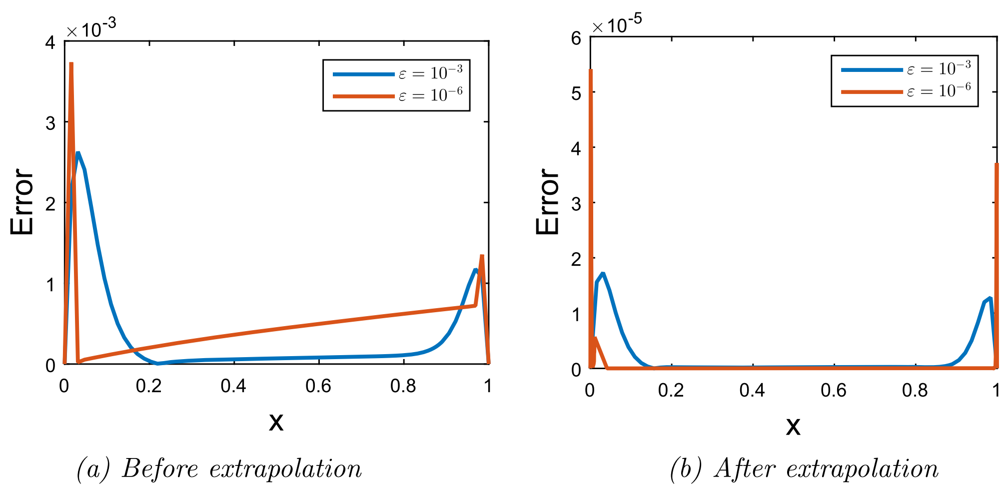

Fig. 3. Error plots on S-mesh for N = 64 of Example 5.1.

For various values of ε, Numerical solutions of Examples 5.1 and 5.2 are plotted in Fig. 1 and 2. These figures display that when ε decreases, boundary layers are present around $x = 0$ and at $x = 1$. On S-mesh, the error is plotted in Fig. 3 of Example 5.1. Similarly, before and after extrapolation, the error is plotted in Fig. 4(a) on the B-S mesh of Example 5.1. From these figures, one can observe that the error is less on the B-S mesh compared to the S-mesh, as well as using the extrapolation method. Before extrapolation, Table 1 shows the approximated maximum pointwise errors and Table 2 presents the extrapolation results for Example 5.1 using the suggested technique. Similarly for Example 5.2, before extrapolation results are given in Table 3 and after extrapolation results are given in Table 4. One can observe from these tables before extrapolation the rate of convergence is almost two (up to logarithm factor) on S-mesh, but on B-S mesh, the rate of convergence is two. Similarly, after extrapolation, the rate of convergence is almost four (upto logrithim factor) on S-mesh but on B-S mesh, the rate of convergence is four. The accuracy is better on B-S mesh compared to S-mesh both before extrapolation and after extrapolation. The highest pointwise errors before and after extrapolation are presented in the log-log scale on S-mesh in Fig. 5 to show the numerical sequence of convergence. Similarly, maximum pointwise errors before and after extrapolation are plotted in Fig. 6 on B-S mesh and B-S mesh, respectively.

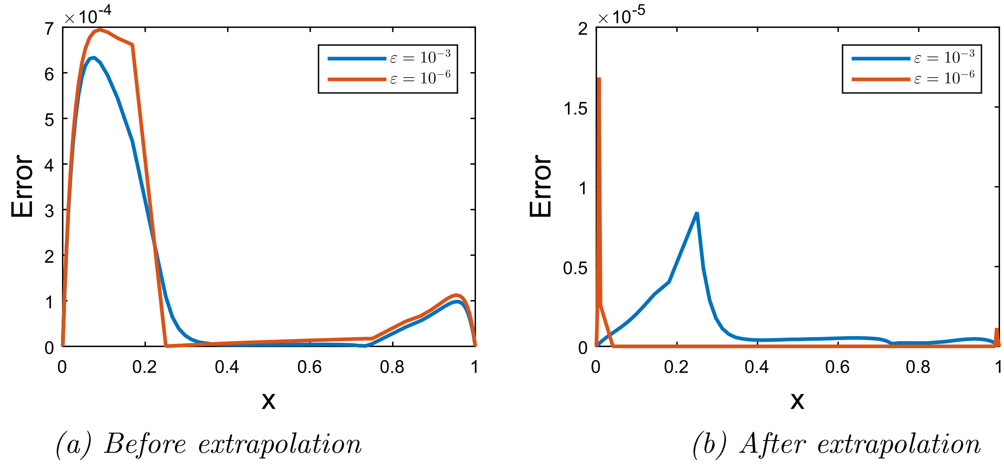

Fig. 4. Error plots on B-S Mesh for N = 64 of Example 5.1.

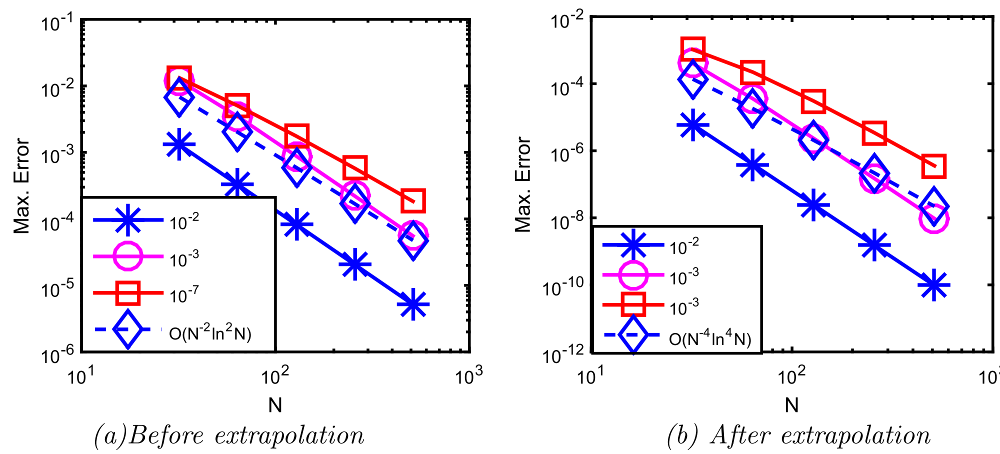

Fig. 5. Loglog plots on S-mesh of Example 5.2.

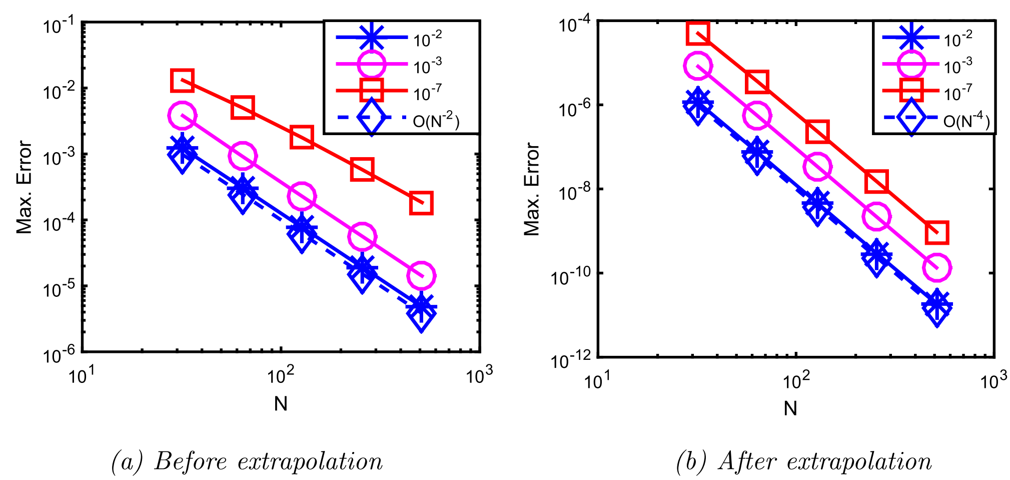

Fig. 6. Loglog plots on B-S mesh of Example 5.2.

6. Conclusion

In this article, the singularly perturbed Fredholm integro-differential equation is solved numerically. The central difference scheme used for the derivative and trapezoidal rule is taken for an integral part of non-uniform meshes (Shishkin mesh, Bakhvalov-Shishkin). We prove that the numerical scheme converges uniformly with respect to the small parameter ε and this method gives second-order accuracy. Then we use the post-processing technique to change the second-order rate of convergence to the fourth-order rate of convergence. Finally, the numerical scheme is tested with two examples. In the future, we develop numerical methods such as the finite element method, hybrid scheme, and finite volume method to solve singularly perturbed Fredholm integro-differential equations.

Table 1
$\widehat{E}_{\varepsilon}^{N}$ and $\widehat{P}_{\varepsilon}^{N}$ using the proposed approach for Example 5.1.

	ε	Number of intervals N				
		32	64	128	256	512
S-mesh	$1e-2$	9.8213e-4	2.4726e-4	6.2045e-5	1.5518e-5	3.8805e-6
		1.9899	1.9946	1.9994	1.9996	2.0000
	$1e-3$	9.1334e-3	2.6290e-3	6.7023e-4	1.6839e-4	4.2151e-5
		1.3967	1.5093	1.6044	1.6553	1.6939
	$1e-4$	3.5840e-4	5.2787e-5	6.5648e-6	7.1345e-7	7.1878e-8
		1.3967	1.5093	1.6044	1.6553	1.6939
	$1e-5$	9.4238e-3	3.5813e-3	1.2583e-3	4.1386e-4	1.3139e-4
		1.3958	1.5090	1.6042	1.6553	1.6939
	$1e-6$	9.4464e-3	3.5906e-3	1.2616e-3	4.1497e-4	1.3174e-4
		1.3955	1.5090	1.6042	1.6553	1.6939
	$1e-7$	9.4536e-3	3.5936e-3	1.2627e-3	4.1532e-4	1.3186e-4
		1.3954	1.5089	1.6042	1.6553	1.6939
	$1e-8$	9.4558e-3	3.5945e-3	1.2630e-3	4.1543e-4	1.3189e-4
		1.3954	1.5089	1.6042	1.6553	1.6939
BS-mesh	$1e-2$	6.6686e-4	1.6773e-4	4.2342e-5	1.0612e-5	2.6547e-6
		1.9913e+00	1.9859e	1.9964	1.9991	1.9998e+00
	$1e-3$	2.6621e-3	6.3340e-4	1.5628e-4	3.8934e-5	9.7248e-6
		2.0714	2.0190	2.0050	2.0013	2.0003e+00
	$1e-4$	2.7957e-3	6.7857e-4	1.6936e-4	4.2398e-5	1.0577e-5
		2.0426	2.0024	1.9980	2.0030	2.0245e+00
	$1e-5$	2.8771e-3	6.9030e-4	1.7172e-4	4.3031e-5	1.0784e-5
		2.0593	2.0072	1.9966	1.9965	1.9981
	$1e-6$	2.9107e-3	6.9469e-4	1.7263e-4	4.3240e-5	1.0834e-5
		2.0669	2.0087	1.9972	1.9967	1.9978
	$1e-7$	2.9215e-3	6.9612e-4	1.7293e-4	4.3309e-5	1.0851e-5
		2.0693	2.0092	1.9974	1.9968	1.9978
	$1e-8$	2.9249e-3	6.9658e-4	1.7302e-4	4.3330e-5	1.0856e-5
		2.0700	2.0093	1.9975	1.9968	1.9978

Table 2
$\widehat{E}_{\varepsilon}^{N}$ and $\widehat{P}_{\varepsilon}^{N}$ using the proposed approach after extrapolation for Example 5.1.

ε		Number of intervals N				
		32	64	128	256	512
S-mesh	$1e-2$	1.4260e-8	8.9625e-10	5.6071e-11	6.7235e-12	3.4941e-11
		3.8718	3.9860	3.9922	3.9938	3.4414
	$1e-3$	2.4776e-4	1.7305e-5	1.1253e-6	7.1284e-8	4.4645e-9
		3.8397	3.9428	3.9806	3.9970	3.9977
	$1e-4$	3.5840e-4	5.2787e-5	6.5648e-6	7.1345e-7	7.1878e-8
		2.7633	3.0074	3.2019	3.3112	3.3886
	$1e-6$	3.6619e-4	5.4108e-5	6.7317e-6	7.3151e-7	7.3709e-8
		2.7587	3.0068	3.2020	3.3110	3.3883
	$1e-7$	3.6678e-4	5.4208e-5	6.7444e-6	7.3288e-7	7.3848e-8
		2.7583	3.0068	3.2020	3.3109	3.3883
	$1e-8$	3.6697e-4	5.4240e-5	6.7484e-6	7.3332e-7	7.3892e-8
		1.9105	2.7582	3.0067	3.2020	3.3109
BS-mesh	$1e-2$	1.1392e-6	7.3403e-8	4.6237e-9	2.8950e-10	1.8509e-11
		3.9561	3.9887	3.9974	3.9673	
	$1e-3$	8.1906e-6	5.4225e-7	3.4157e-8	2.1390e-9	1.3386e-10
		3.9169	3.9887	3.9972	3.9982	
	$1e-4$	1.4258e-4	9.5417e-6	6.0709e-7	3.8116e-8	2.3851e-9
		3.9014	3.9743	3.9934	3.9983	
	$1e-6$	4.9732e-5	3.5400e-6	2.3298e-7	1.4844e-8	8.3848e-9
		3.8124	3.9255	3.9723	8.2400e-01	
	$1e-7$	4.9891e-5	3.5505e-6	2.3370e-7	1.4875e-8	9.3814e-10
		3.8127	3.9253	3.9737	3.9870	
	$1e-8$	4.9942e-5	3.5538e-6	2.3394e-7	1.4890e-8	9.3889e-10
		3.8128	3.9252	3.9737	3.9872	

Availability of supporting data

Not applicable.

Funding

This work was financially supported by the Research Center of Energy Conservation for New Generation of Residential, Commercial, and Industrial Sectors of National Taipei University of Technology within the framework of the Higher Education Sprout Project by the Ministry of Education (MOE) in Taiwan.

Author's contributions

All the authors contributed equally and significantly to writing this article and typed, read, and approved the final manuscript.

Table 3
$\widehat{E}_{\varepsilon}^{N}$ and $\widehat{P}_{\varepsilon}^{N}$ using the proposed approach for Example 5.2.

	ε	Number of intervals N				
		32	64	128	256	512
S-mesh	$1e-2$	1.2946e-3	3.2795e-4	8.2527e-5	2.0649e-5	5.1633e-6
		1.9809	1.9905	1.9988	1.9997	
	$1e-3$	1.1999e-2	3.4559e-3	8.8154e-4	2.2152e-4	5.5451e-5
		1.7958	1.9710	1.9926	1.9981	
	$1e-4$	1.2829e-2	4.8658e-3	1.7114e-3	5.6305e-4	1.7873e-4
		1.3987	1.5075	1.6039	1.6555	
	$1e-5$	1.3074e-2	4.9658e-3	1.7452e-3	5.7403e-4	1.8222e-4
		1.3966	1.5087	1.6042	1.6554	
	$1e-6$	1.3149e-2	4.9966e-3	1.7556e-3	5.7741e-4	1.8330e-4
		1.3960	1.5090	1.6043	1.6554	
	$1e-7$	1.3173e-2	5.0063e-3	1.7588e-3	5.7847e-4	1.8364e-4
		1.3958	1.5091	1.6043	1.6554	
	$1e-8$	1.3180e-2	5.0093e-3	1.7599e-3	5.7880e-4	1.8375e-4
		1.3957	1.5092	1.6043	1.6554	
BS-mesh	$1e-2$	1.2179e-3	3.0708e-4	7.6716e-5	1.9184e-5	4.7960e-6
		1.9878	2.0010	1.9996	2.0000	
	$1e-3$	3.8127e-3	9.1627e-4	2.2661e-4	5.6471e-5	1.4106e-5
		2.0570	2.0156	2.0046	2.0012	
	$1e-4$	3.9084e-3	9.5114e-4	2.3753e-4	5.9567e-5	1.4878e-5
		2.0389	2.0016	1.9955	2.0013	
	$1e-5$	3.9900e-3	9.5959e-4	2.3894e-4	5.9900e-5	1.5017e-5
		2.0559	2.0058	1.9960	1.9959	
	$1e-6$	4.0382e-3	9.6449e-4	2.3973e-4	6.0056e-5	1.5049e-5
		2.0659	2.0084	1.9970	1.9966	
	$1e-7$	4.0537e-3	9.6611e-4	2.4002e-4	6.0115e-5	1.5062e-5
		2.0690	2.0090	1.9974	1.9968	
	$1e-8$	4.0587e-3	9.6663e-4	2.4011e-4	6.0134e-5	1.5067e-5
		2.0700	2.0093	1.9975	1.9968	

Table 4
$\widehat{E}_{\varepsilon}^{N}$ and $\widehat{P}_{\varepsilon}^{N}$ using the proposed approach after extrapolation for Example 5.2.

	ε	Number of intervals N				
		32	64	128	256	512
S-mesh	$1e-2$	6.0575e-6	3.8767e-7	2.4376e-8	1.5256e-9	9.5663e-11
		3.9658	3.9913	3.9980	3.9953	
	$1e-3$	4.0055e-4	3.5250e-5	2.3450e-6	1.5115e-7	9.4846e-9
		3.5063	3.9099	3.9555	3.9943	
	$1e-4$	2.7742e-3	8.7988e-4	1.7186e-4	1.3685e-5	9.3259e-7
		1.6567	2.3561	3.6505	3.8753	
	$1e-6$	1.0446e-3	2.1996e-4	3.0533e-5	3.4924e-6	3.5617e-7
		2.2477	2.8488	3.1281	3.2936	
	$1e-7$	1.0469e-3	2.1983e-4	3.0527e-5	3.4916e-6	3.5608e-7
		2.2517	2.8482	3.1281	3.2936	
	$1e-8$	1.0476e-3	2.1979e-4	3.0525e-5	3.4914e-6	3.5605e-7
		2.2529	2.8481	3.1281	3.2937	
B-S-mesh	$1e-2$	1.1392e-06	7.3403e-8	4.6237e-9	2.8950e-10	1.8509e-11
		3.9561	3.9887	3.9974	3.9673	
	$1e-3$	8.1906e-6	5.4225e-7	3.4157e-8	2.1390e-9	1.3386e-10
		3.9169	3.9887	3.9972	3.9982	
	$1e-4$	1.4258e-4	9.5417e-6	6.0709e-7	3.8116e-8	2.3851e-9
		3.9014	3.9743	3.9934	3.9983	
	$1e-6$	4.9732e-5	3.5400e-6	2.3298e-7	1.4844e-8	8.3848e-9
		3.8124	3.9255	3.9723	8.2400	
	$1e-7$	4.9891e-5	3.5505e-6	2.3370e-7	1.4875e-8	9.3814e-10
		3.8127	3.9253	3.9737	3.9870	
	$1e-8$	4.9942e-5	3.5538e-6	2.3394e-7	1.4890e-8	9.3889e-10
		3.8128	3.9252	3.9737	3.9872	

Ethical approval

Not applicable.

Declaration of competing interest

The authors declare that they have no competing interests concerning the publication of the manuscript.

References

[1] G.M. Amiraliyev, M.E. Durmaz, M. Kudu, Uniform convergence results for singularly perturbed Fredholm integro-differential equations, J. Math. Anal. 9 (6) (2018) 55–64.

[2] D. Baleanu, S. Arshad, A. Jajarmi, W. Shokat, F.A. Ghassabzade, M. Wali, Dynamical behaviours and stability analysis of a generalized fractional model with a real case study, J. Adv. Res. 48 (2023) 157–173.

[3] D. Baleanu, M. Hasanabadi, A.M. Vaziri, A. Jajarmi, A new intervention strategy for an HIV/AIDS transmission by a general fractional modeling and an optimal control approach, Chaos Solitons Fractals 167 (2023) 113078.

[4] H. Brunner, P. van der, The Numerical Solution of Volterra Equations CWI Monographs, NorthHolland, Amsterdam, 1986.

[5] J. Chen, M. He, T. Zeng, A multiscale Galerkin method for second-order boundary value problems of Fredholm integro-differential equation II: efficient algorithm for the discrete linear system, J. Vis. Commun. Image Process. 58 (2019) 112–118.

[6] J. Chen, M. He, Y. Huang, A fast multiscale Galerkin method for solving second order linear Fredholm integro-differential equation with Dirichlet boundary conditions, J. Comput. Appl. Math. 64 (2020) 112352.

[7] Vincenzo Ciancio, Derivations of the stress-strain relations for viscoanelastic media and the heat equation in irreversibile thermodynamic with internal variables, Int. J. Math. Comput. Eng. 2 (2) (2024) 1–14.

[8] E. Cimen, M. Cakir, A uniform numerical method for solving singularly perturbed Fredholm integro-differential problem, Comput. Appl. Math. 40 (42) (2021) 1–14.

[9] A. De Gaetano, O. Arino, Mathematical modelling of the intravenous glucose tolerance test, J. Math. Biol. 40 (2000) 136–168.

[10] G. De Marsily, Quantitative Hydrogeology-Groundwater Hydrology for Engineers, Academic Press, New York, 1986.

[11] M.E. Durmaz, G.M. Amiraliyev, A robust numerical method for a singularly perturbed Fredholm integro-differential equation, Mediterr. J. Math. 18 (24) (2021) 1–17.

[12] M.E. Durmaz, I. Amirali, G.M. Amiraliyev, An efficient numerical method for a singularly perturbed Fredholm integro-differential equation with integral boundary condition, J. Appl. Math. Comput. (2022) 1–24.

[13] D. Green, H.W. Stech, Diffusion and Hereditary Effects in a Class of Population Models, Differential Equations and Applications in Ecology, Epidemics, and Population Problems, Academic Press, New York-London, 1981, pp. 19–28.

[14] R. Jalilian, T. Tahernezhad, Exponential spline method for approximation solution of Fredholm integro-differential equation, Int. J. Comput. Math. 97 (4) (2020) 791–801.

[15] A. Jerri, Introduction to Integral Equations with Applications, Wiley, New York, 1999.

[16] M. Kudu, I. Amirali, G.M. Amiraliyev, A finite-difference method for a singularly perturbed delay integro-differential equation, J. Comput. Appl. Math. 308 (2016) 379–390.

[17] C.G. Lange, D.R. Smith, Singular perturbation analysis of integral equations: part II, Stud. Appl. Math. 90 (1) (1993) 1–74.

[18] X. Liu, M. Yang, Error estimations in the balanced norm of finite element method on Bakhvalov–Shishkin triangular mesh for reaction–diffusion problems, Appl. Math. Lett. 123 (2022) 107523.

[19] A.S. Lodge, J.B. McLeod, J.A.A. Nohel, Nonlinear singularly perturbed Volterra integro differential equation occurring in polymer rheology, Proc. R. Soc. Edinb., Sect. A 80 (1978) 99–137.

[20] J.J.H. Miller, E. O'Riordan, I.G. Shishkin, Fitted Numerical Methods for Singular Perturbation Problems, World Scientific, Singapore, 2012.

[21] J. Mohapatra, L. Govindarao, A fourth order optimal numerical approximation and its convergence for singularly perturbed time delayed parabolic problems, Iran. J. Numer. Anal. Optim. (2021), https://doi.org/10.22067/IJNAO.2021.71891.1053.

[22] J. Mohapatra, S. Natesan, Uniformly convergent second-order numerical method for singularly perturbed delay differential equations, Neural Parallel Sci. Comput. 16 (3) (2008) 353.

[23] M. Mulimani, K. Srinivasa, A novel approach for Benjamin-Bona-Mahony equation via ultraspherical wavelets collocation method, Int. J. Math. Comput. Eng. 2 (2) (2024) 39–52.

[24] M.C. Natividad, M. Stynes, An extrapolation technique for a singularly perturbed problem on Shishkin mesh, in: Proceedings of the Third Asian Mathematical Conference 2000, 2002, pp. 383–388.

[25] N.N. Nefedov, A.G. Nikitin, The Cauchy problem for a singularly perturbed integro-differential Fredholm equation, Comput. Math. Math. Phys. 47 (4) (2007) 629–637.

[26] V. Raja, E. Sekar, S. Shanmuga Priya, B. Unyong, Fitted mesh method for singularly perturbed fourth order differential equation of convection diffusion type with integral boundary condition, AIMS Math. 8 (7) (2023) 16691–16707.

[27] V. Raja, A. Tamilselvan, G.J. Jayalakshmi, E. Sekar, Fitted finite difference technique for singularly perturbed reaction diffusion equations of third order with integral boundary condition, Int. J. Numer. Methods Fluids, https://doi.org/10.1002/fld.5201, 2023.

[28] A. Saadatmandi, M. Dehghan, Numerical solution of the higher-order linear Fredholm integro-differential-difference equation with variable coefficients, Comput. Math. Appl. 59 (2010) 2996–3004.

[29] E. Sekar, Second order singularly perturbed delay differential equations with non-local boundary condition, J. Comput. Appl. Math. 417 (2023) 114498.

[30] E. Sekar, A. Tamilselvan, Singularly perturbed delay differential equations of convection–diffusion type with integral boundary condition, J. Appl. Math. Comput. 59 (1) (2019) 701–722.

[31] E. Sekar, A. Tamilselvan, Parameter uniform method for a singularly perturbed system of delay differential equations of reaction–diffusion type with integral boundary conditions, Int. J. Appl. Math. 5 (3) (2019) 1–12.

[32] E. Sekar, A. Tamilselvan, R. Vadivel, Nallappan Gunasekaran, Haitao Zhu, Jinde Cao, Xiaodi Li, Finite difference scheme for singularly perturbed reaction diffusion problem of partial delay differential equation with non local boundary condition, Adv. Differ. Equ. 1 (2021) 1–20.

[33] Elango Sekar, Bundit unyong, numerical scheme for singularly perturbed mixed delay differential equation on Shishkin type meshes, Fractal Fract. 7 (1) (2023) 43.

[34] G.I. Shishkin, L.P. Shishkina, Difference Methods for Singular Perturbation Problems, CRC Press, Boca Raton, 2009.